A STUDY ON HYDRAULIC PRESSURE ACTING ON A SLUICE-GATE

Dr. Eng., Masashi HOM-MA, C.E. Member, Shin-ichi SENSHU, C.E. Member,***
*and Akihiko TSUCHIYA, C.E. Assoc. Member****

1. INTRODUCTION

Some research papers on the same problem have already been published[1] and the general properties of the pressure are made clear by the analyses and the experiments, while the authors intended to know through this research the character of hydraulic pressure on gate leaves when the openings of gates are very small. Usually the uplift force acting on a gate-leaf growths rapidly when the leaf-lip approaches very near to the surface of sill. Giving the explanation of this tendency is the main object of this experimental research.

Fig. 1

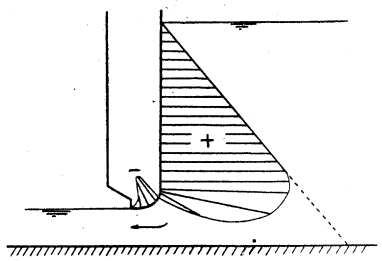

A typical distribution of pressure along the profile of gate-leaf with rounded corner is shown in the **fig. 1**. From this sort of figures we can estimate the horizontal and vertical components (H and V say) of the total pressure. The main elements which may affect the amount of H or V, above defined, are; the water depth in the upper reach of the gate (h), the gate opening (a), the radius of rounded corner of lip (R) and the width of sealing part (s). As will be shown in the following articles, the amounts of hydraulic pressure, especially of the vertical component V, differ each other according the states of outflowing nappe, which are classified by the authors into two cases; those are

Case A : Perfectly adhered nappe (**fig. 2, A**).

Case B : Partially separated nappe (**fig. 2, B**).

Among the above mentioned elements affecting the pressure distribution, the length s seems to have no essential effect as far as this length remains in a certain limit. The authors, therefore, investigate the pressure distribution in the ralation with a/h or R/h, for the two **cases A** and **B** respectively.

Fig. 2

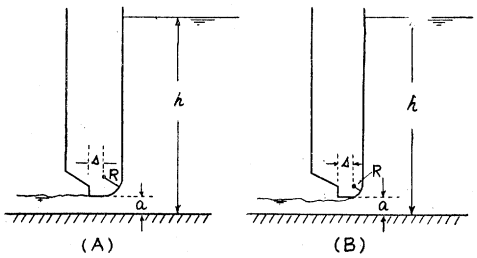

Write H_0 and V_0 for the amount of H and V in the state of perfect closure and also write

$$H=H_0-\delta H, \qquad V=V_0-\delta V$$

for the state of partial opening, then the measured values of H and V will give δH and δV respectively, using the computed amounts of H_0 and V_0 for the given values of h and R.

2. TEST MODELS

Two flumes of different scales were prepared for this research.

(1) Large scale test The system of the test flume is shown in the following scheme.

* Professor, Faculty of Engineering, University of Tokyo
** Technical Institute of Electric Power
*** Public Works Research Institute, Ministry of Construction.

Head tank ⟶ Measuring weir ⟶ Flow regulating tank ⟶ Main tank ⟶ Gate model
(97×160×195) (Rectangular 32×46) (100×120×100) (200×30×230)
↑ Pump ⟵ Pool ⟵ Lower tank ⟵ Tail channel ⟵
(100×80×75) (30×30×270)

(The dimension of tank is; Height×Breadth×Length in cm unit).

The main tank is made of wood, reinforced from the outside by steel angles and bolts to bear the water head of 2 m. A part of wooden side wall along which the gate lip moves is replaced by a sheet of thick glass (20×100), so that the outflow nappe from the model lip can be observed. The model gate is set up at the position of lower end of main tank on the horizontal sill. The gate leaf is a hard-wood board of 3×30×200 size, and it is equipped with one of the lips, their dimensions being shown in the **figure 3**. This leaf moves along steel railings fixed on the side walls above the upper edge of glass window. The lip is provided with rubber sheets to prevent the leakage.

Fig. 3

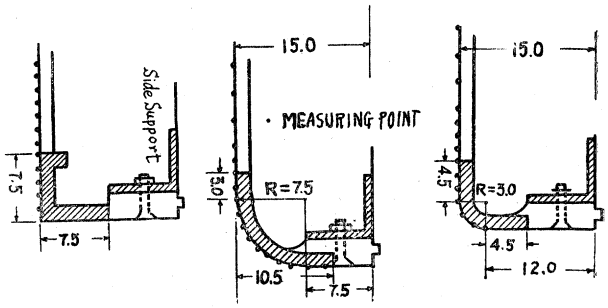

For the small amount of gate opening (a), the outflow discharge (Q) may be expressed by

(1) $$Q=\mu a\sqrt{2gh},$$

where μ is the outflow coefficient and the values of μ computed from the observed data are formularized as shown in the following table.

Dimension of lip		Range of experiment		μ (m-sec unit)
R(cm)	s(cm)	a(cm)	h(m)	
0	7.5	1.0—8.0	0.2—2.0	$0.581\,h^{0.018}$
		(for $a<1.0$, the nappe of outflow jet is unstable).		
7.5	3.0	0.5—6.0	0.2—2.0	$0.932\,h^{0.028}$
3.0	4.5	0.5—2.4	0.2—2.0	$0.955\,h^{0.0031}$
3.0	4.5	2.4—6.0	0.2—2.0	$(0.463/a^{0.1935})h^{0.0035}$

(2) Small scale test The scheme of this model system is as following.

Head tank ⟶ Gate model ⟶ Steel framed glass channel ⟶
(50×60×60) (45×26×0.2) (30×40×120) ↓
↑ Pump ⟵ Lower tank ⟵ Measuring tank with triangular notch

The gate leaf is a steel plate provided with one of the lips shown in the **figure 4**, and it is operated by a handle and a rod screw. The effective outflow width under the lip is 24 cm.

The computed outflow coefficients μ for these gate lips are formularized like the former case.

Dimension of lip		Range of observation		μ (cm-sec unit)
R(cm)	s(cm)	a(cm)	h(cm)	
1.0	4.0	0.1	10—40	$0.921\,h^{-0.018}$
1.0	4.0	0.2—0.4	10—40	$0.849\,h^{0.042}$
3.0	2.2	0.2	10—40	$0.668\,h^{0.060}$
3.0	2.2	0.3—0.6	10—40	$0.922\,h^{0.053}$

3. RESULTS OF THE EXPERIMENT

(1) Typical distribution of pressure and hydraulic numbers

The pressure distribution was observed for each case and from their results H and V were com-

Fig. 4

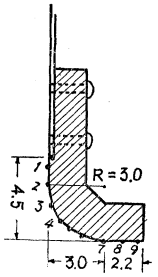

Fig. 5

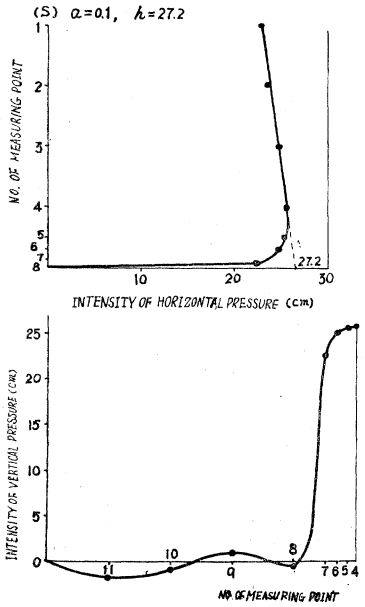

Fig. 6

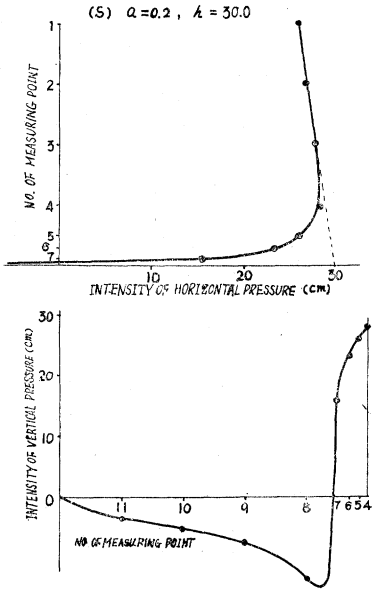

puted graphically. The **figures 5** and **6** show two examples of the small scale test; those are the cases of $R=1.0$, $a=0.1$, $h=27.2$, and $R=1.0$, $a=0.2$, $h=30.0$ (in cm unit). They show that the opening of gate has much larger effect on vertival component than on horizontal component.

The Reynolds' number can be written as

(2) $$R_e=va/\nu=\sqrt{2gh}\cdot a/\nu$$

where v is the mean outflow velocity. The ranges of the value of R_e in this experiment are; 35,000-500,0000 for the large scale test, and 1,400-17,000 for the small scale test.

The cavitation coefficient K is written as

(2) $$K=\frac{p_0-p_v}{\rho v^2/2}=\frac{p_0-p_v}{\rho g}\frac{2g}{v^2}=\left(1{,}000-\frac{p_v}{\rho g}\right)\frac{1}{h}$$

where p_0 and p_v are intensities of atmospheri pressure and vapour tension respectively, and the unit of length is cm. The value of $p_v/\rho g$ is about 20 cm for 15-20°C. Then the approximate lower limits of K in this experiment are; nearly 5 for the large scale test and above 30 for the small scale test. In the equation (3), $\sqrt{2gh}$ is taken for v instead of the local velocity along the curved surface. If the local velocity exceeds twice of the mean velocity, the value of K for the large model may become nearly 1. This means that the occurence of cavitation is possible.

(2) Flow in the state A (Perfectly adhered) In the experiment of large scale model, the lip of $R=7.5$ cm produces the state A for the whole range of observation. But the curves of pressure distribution are not similar each other. The following table gives the approximate depth h which produces the maximum absolute value of negative pressure on the corner of lip surface for each opening.

R=7.5 cm, h=1.0—2.0 m

a cm =	0.5	1.0	1.55	2.0	3.0	3.5	4.5	5.0
h m ≒	1.0	1.3	1.5	2.0	2.0	1.8	1.2	1.0

The surface of separated nappe is very unstable and is not easily distinguishable. It is only supposed from the curves of pressure distribution that the outflow from the lip of R=3.0 cm in large model makes adhered nappe when a/h is faily large for any constant opening. In the small model, the distinction of flow state is more difficult than the former case, but it is supposed that lip of R=3.0 cm produces the state A in the whole range, and the outflow from the lip of R=1.0 cm is nearly in the transient region of the two states.

To find out the characters of pressure from the observed data, the authors assumed the relation

$$\delta H/H_0 = f(a/h,\ h/R)$$

neglecting the effect of s on H or V, and gave the following figures. (**Fig. 7～9**)

In the **figure 9**, the relation is represented by a family of curves which has a parameter h (if the value of a is prefered as the parameter, the curves become slightly upward concave), while in the **figure 7** all curves lie nearly on one straight line. The slope of curve is larger for the small model than the

Fig. 7
Small scale, R=3.0 cm, $\delta H/H_0$ versus a/h

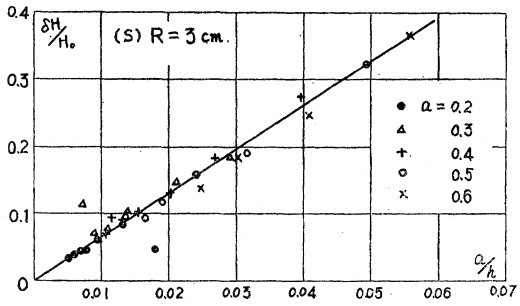

Fig. 8 Small scale, R=3.0 cm, $\delta H/H_0$ versus a/R

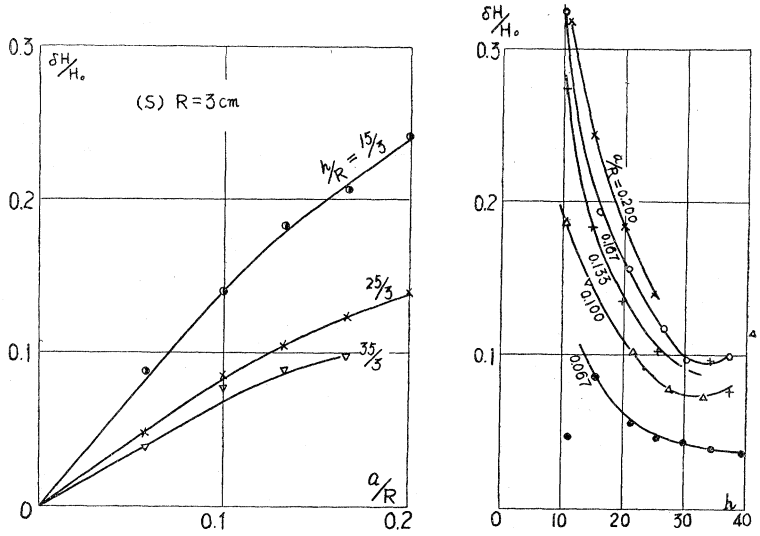

Fig. 9
Large scale, R=7.5 cm, $\delta H/H_0$ versus a/h

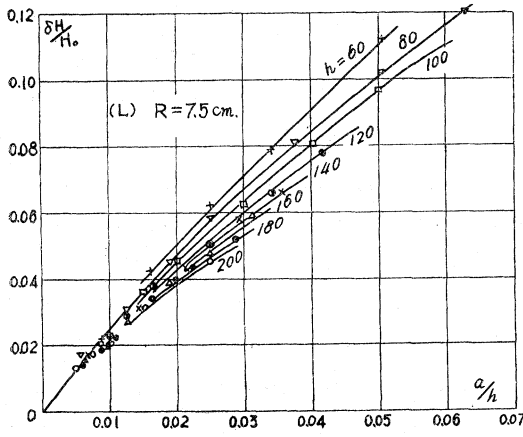

Fig. 10
Small scale, R=1.0 cm, $\delta H/H_0$ versus a/H

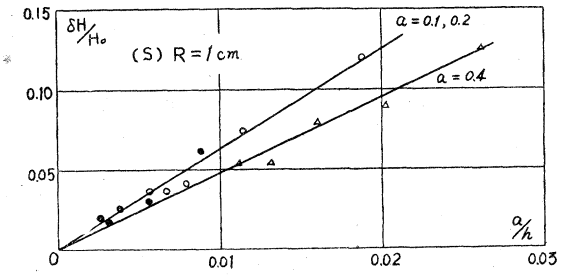

other. The relation of $\delta H/H_0$ versus a/R in the **fig. 8** is made by the curves in the right-hand side of this figure. Now there is given a relation for a smaller radius of lip profile in the **figure 10.**

The relations are represented by approximately straight lines which have smaller slopes than that of the **fig. 7.**

Concerning the vertical force, the authors gave the following figures. (**Fig. 11~13**)

These results show that the change of uplift force mainly depends on the amount of a, not on h. The broken line in the **fig. 12** is the result of semi- theoretical calculation by the equi-velocity arc method. The curves in the **fig. 13** are fairly regular and this fact suggests that the flow from the lip of $R=1.0$ cm is nearly in the state A. For the region of $a/R>0.05$ in the **fig. 11** or $a/R>0.15$ in the **fig. 13**, the amount of $\delta V/V_0$ exceeds unity, that means the vertical force V in such case is negative, or, in the other words, of downwards direction. On the contrary the experiment of large model does not give any negative amount of V. The reason will be discussed later on.

Fig. 11 Small scale, $R=3.0$ cm, $\delta V/V_0$ versus a/R

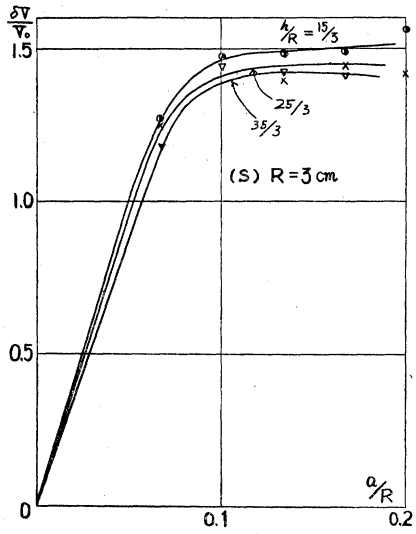

Fig. 12
Large scale, $R=7.5$ cm, $\delta V/V_0$ versus a/R

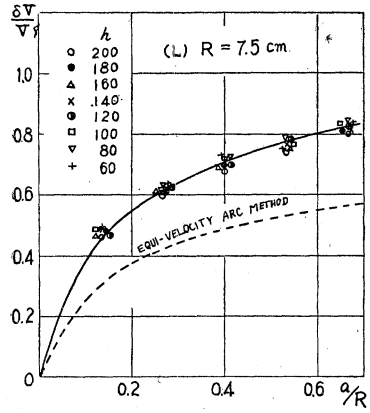

Fig. 13
Small scale, $R=1.0$ cm, $\delta V/V_0$ versus a/R

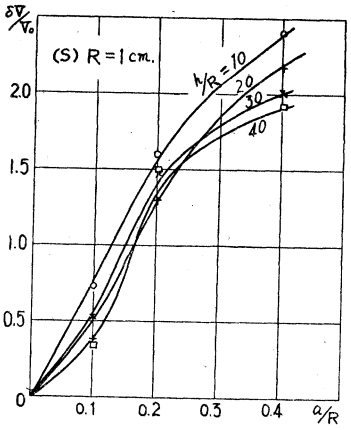

Fig. 14
Large scale, $R=3.0$ cm, $\delta H/H_0$ versus a/h

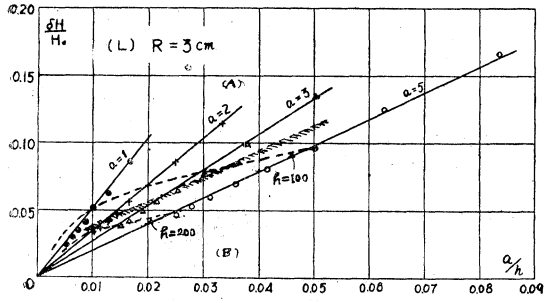

(3) Flow in the state B (Separated nappe)

As already stated, the lip of $R=3.0$ cm in the large scale model seems to produce the flow state B for a wide range of a/h. The following two figures show the relation between $\delta H/H_0$ and a/h for the state B. (**Fig. 14~15**)

Broken lines in the **fig. 14** are the curves

Fig. 15
Large scale, $R=0$ cm

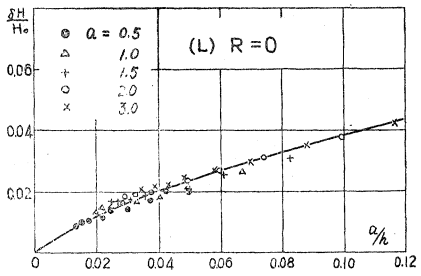

when h is taken as the parameter, and the shaded zone shows the limit of region where the flow is in the state B. The flow stage is so unsteady that $\delta V/V_0$ fluctuates too much to show any definite tendency. For the lip of $R=0$, the separation point of nappe is again fixed and the state of flow becomes very stable.

4. ANALYSES OF HYDRAULIC PRESSURE

Concerning the outflow under a sharp-edged gate, we can see that the analytical methods[2] give fairly good results, while for the gate with a curved lip only approximate methods may be applied. In this research the authors adopted the following two methods.

(1) Method of circular equi-velocity arcs The authors applied the method shown in the book of Koch-Carstanjen[3] to the case of curved lips and assumed the circular equi-velocity arcs as shown in the **fig. 16**. O is the common center of the arcs which ends on the straight wall, while O′, O″,……are the centers of arcs which end on the curved part of wall.

Fig. 16

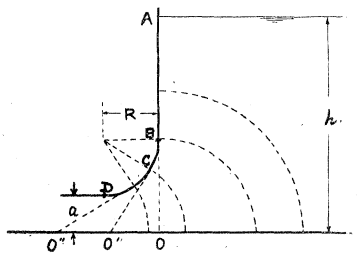

The horizontal component H introduced from this assumption is given by the following equation, with the notations shown in the figure

$$H=w\frac{(h-a)^2}{2}-w\frac{(\mu a)^2}{h}\left[a-h+\frac{4h^2}{\pi^2(R+a)}-\frac{4h}{\pi^2}-\left(\frac{h}{a}\right)^2 R\int_0^{\pi/2}F_1\left(\frac{R}{a},\ \alpha\right)d\alpha\right] \tag{4}$$

where w is the unit weight of water and

$$\mu=\frac{Q}{a\sqrt{2gh}},\quad F_1=\cos^3\alpha\left(\frac{\pi}{2}-\alpha\right)^{-2}\left\{1+\frac{R}{a}(1-\sin\alpha)\right\}^{-2},$$

The vertically upward component V is also given by

$$V=wR\left\{h-a-\left(1-\frac{\pi}{4}\right)R\right\}-w\left\{\left(\frac{h}{a}\right)^2\int_0^{\pi/2}F_2\left(\frac{R}{a},\ \alpha\right)d\alpha-1\right\}\frac{R(\mu a)^2}{h} \tag{5}$$

where $F_2=F_1\cdot\tan\alpha$.

The equation (5) does not include the pressure acting on the sealing part of length s. The definite integrals in these equations are given from the **fig. 17**. Dividing the discharge Q by the length of circular arc in the **fig. 16**, we gain the velocity in any point. Thus we can culculate the velocity- and pressure-head along the surface of gate.

Fig. 17

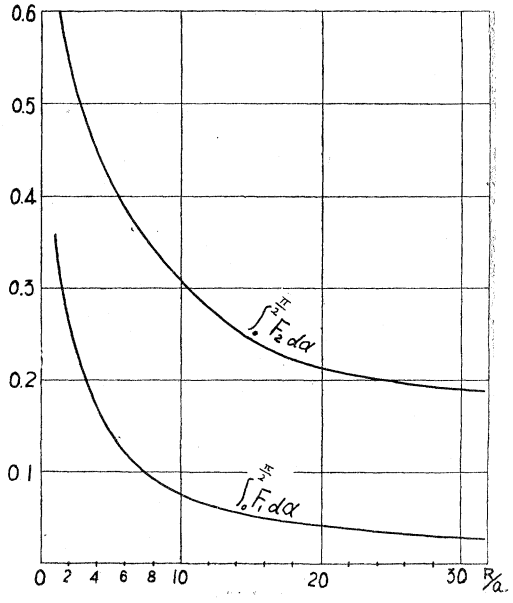

Example 1. The given data are (in c.g.s. units), $R=3.0$, $a=0.5$, $h=30.0$ for the small model. From

the given value of μ, $Q=\mu a\sqrt{2gh}=130.5$ cc/s/cm. Substituting these into the eq. (4), we get $H=434.65$, from which $\delta H=[w(h-a)^2/2]-H=435.60$ gr/cm.

The vertical component is computed from the eq. (5), that is $V=45.90$. Then $V_0=(h-a)R-1.93=86.57$, $\delta V=40.67$, $\delta V/V_0=0.41$. The distribution of pressure is shown in the figure 21.

(2) Method of stream line analysis At first the principle of the method proposed by Uchida[4] is explained briefly.

If we adopt a set of orthogonal coordinates α and β, the velocity components u and v are given by

$$u=\frac{1}{h_\beta}\frac{\partial\psi}{\partial\beta},\quad v=-\frac{1}{h_\alpha}\frac{\partial\psi}{\partial\alpha},\quad \psi:\text{stream function,} \tag{6}$$

using current coordinates h_α, h_β[5]. For the irrotational motion the equation

$$\frac{\partial}{\partial\alpha}\left(\frac{h_\beta}{h_\alpha}\frac{\partial\psi}{\partial\alpha}\right)+\frac{\partial}{\partial\beta}\left(\frac{h_\alpha}{h_\beta}\frac{\partial\psi}{\partial\beta}\right)=0 \tag{7}$$

must hold. If we draw the lines of $\beta=$const. to coincide approximately with the stream lines as near as possible to real ones (see **fig. 18**), $\partial\psi/\partial\alpha$ is nearly 0 along the line of $\beta=$const. and $\partial\psi/\partial\beta$ is nearly constant along the line $\alpha=$const., that is

Fig. 18

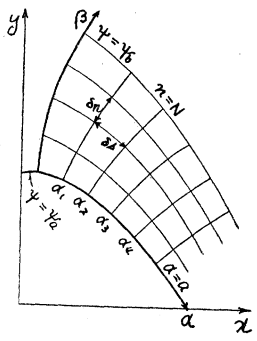

$$\frac{\partial}{\partial\beta}\left(\frac{h_\alpha}{h_\beta}\frac{\partial\psi}{\partial\beta}\right)=0 \tag{8}$$

This equation gives the $(m+1)$th approximation of ψ when the mth approximation of α, h_α and h_β are known. For the numerical calculation we write

$$\frac{h_\alpha}{h_\beta}\frac{\partial\psi}{\partial\beta}=F(\alpha) \tag{9}$$

Then $F(\alpha)$ gives the velocity distribution along the boundary ($\alpha=a$ in the **fig. 18**). If we write the velocity on it as "u_a", the velocity in any point is given by

$$h_a\cdot u=F(\alpha)=h_{\alpha a}\cdot u_a\ . \tag{10}$$

Integrating the expression of u in the eq. (6) from the boundary (β_a) to an arbitrary point β, we will get

$$\psi-\psi_a=\int_{\beta_\alpha}^{\beta}uh_\beta\,d\beta=\int_0^n u\,\delta n, \tag{11}$$

where δn is an length element along the line $\alpha=$const. and equal to $h_\beta d\beta$. We may transform the eq. (11) into a dimensionless from, using U and l as the standard amounts of velocity and length.

$$\frac{\psi}{Ul}-\frac{\psi_a}{Ul}=\int_0^{n/l}\frac{u}{U}\delta\left(\frac{n}{l}\right). \tag{12}$$

For the boundary a, ψ_a may be taken as 0 and for the second boundary we take $n=N$ and $\psi=\psi_b$, then the final equation of u_a is

$$\frac{u_a}{U}=\frac{\psi_b/Ul}{\int_0^{N/l}(\delta s_a/\delta s)\delta(n/l)} \tag{13}$$

where $\delta s_a/\delta s=h_{\alpha a}/h_\alpha$ (δs being a length element along $\beta=$const.). The graphical calculation of the eq. (13) gives u_a, and from the relation $u=u_a(\delta s_a/\delta s)$ the velocity distribution along a potential line may be calculated. To make an adjustment of stream line, we put the computed u in the right-hand side of the eq. (12) and calculate the adjusted value of ψ/Ul. New potential lines are drawn as to

be orthogonal to the adjusted stream lines. This procedure must be repeated.

Fig. 19

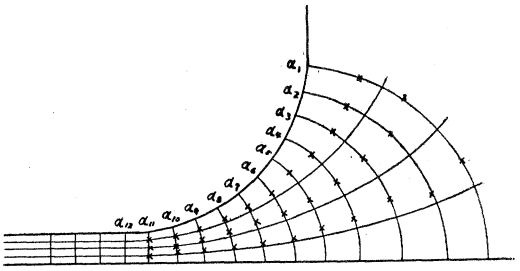

Example 2. The given data are the same with the example 1. At first three stream lines which divide the whole breadth of flow into four equal bands are drawn. The equi-potential lines $\alpha_1 \sim \alpha_{12}$ (see the **fig. 19**) are drawn to make right angle with each stream line. δs and δn for all intersections are measured on the figure and the computed $\delta s_a/\delta s$ and $\delta n/l$ are tab ulated. As the standard amounts l and U, the depth of tank $h=30$ cm and the outflow velocity $\sqrt{2gh}=242.5$ are adopted respectively. This table gives

$$\left(1+\frac{\delta s_a}{\delta s_1}\right)\frac{1}{2}\frac{\delta n_1}{l},\quad \left(\frac{\delta s_a}{\delta s_1}+\frac{\delta s_a}{\delta s_2}\right)\frac{1}{2}\frac{\delta n_2}{l},\quad \cdots\cdots$$

for four intersections on each curve $\alpha_1 \sim \alpha_{12}$. The integral in the eq. (13) is computed as the sum of them, which with $\psi_b=130.5$ gives u_a/U from the eq. (13). $u_1/U, \cdots\cdots u_b/U$ may be computed from u_a and $\delta s_a/\delta s$. The **fig. 20** shows an example of compuled curve of u/U. The integration is performed graphically and the adjusted values of n/l corresponding to $\psi_b/4Ul, \cdots\cdots \psi_b/Ul$ are determined on the figure. The adjusted position of intersections are shown by $\times$ marks in the **fig. 19**. The calculated pressure distribution is plotted in the **fig. 21** with the observed result.

Fig. 20

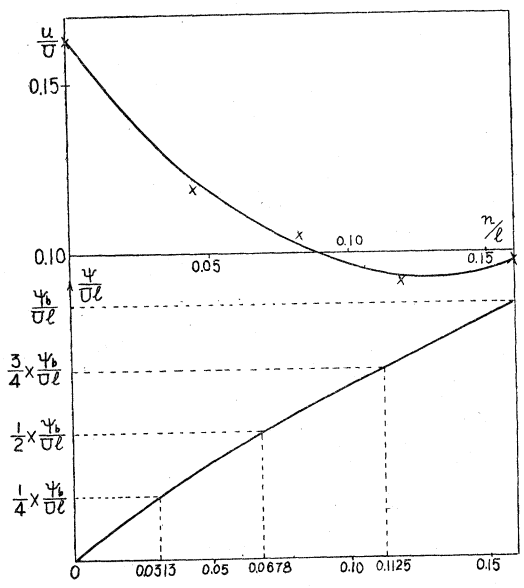

Fig. 21

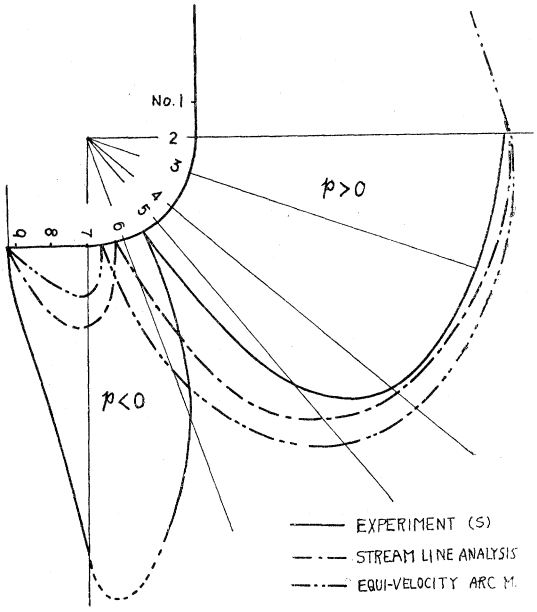

5. CONSIDERATIONS ON THE RESULTS OF EXPERIMENTS AND ANALYSES

It is noticed that the measured pressure is much larger in negative amount than the calculated ones. In this case, cavitation is thought to have not much rôle on the fact. The depth of boundary layer along the lip surface is only about 0.1 mm by the calculation for the case of above example. The authors, at present, think that the cause which is considered to be dominant for the fact is the

neglection of internal friction in their analyses. In the small model the flow is nearly laminar, and the velocity near the lip surface may be much larger than that near the bottom. Perhaps such velocity distribution made the much bigger amount of negative pressure than those by calculations. In the experiment of large model, the effect of fluid resistance is not so remarkable. Therefore the results are not apart far from the observations.

It is apparent for the both models that the uplift force acting on the gate leaf becomes very large for a small gate-opening. It also comes from the remarkable fluid resistance which makes velocity head small and pressure head large. This uplift force may be lessen by making the sealing width s as small as possible in the limit of sealing demand.

The results of the experiment show that the lip with circular corner produces a large amount of negative pressure which causes unsteadiness of flow and fluctuation of nappe. Such faults may be avoided by adopting the profiles proposed by the test at the U.S. Waterways Experiment Station[6].

6. ACKNOWLEDGMENT

The experiment of the large scale model was carried out by S. Senshu in 1953, that of the small scale model and the analytical calculations were performed by A. Tsuchiya in 1955, and the general considerations were given by M. Hom-ma. The authors express their thanks to the Ministry of Construction and the Kansai Denryoku Co. for their helps given to this research.

References;

1) Koch-Carstanjen; Bewegung des Wassers und dabei auftretende krafte. 1926.
O. Mueller; Mitteilungen der Preussischen Versuchsanstalt für Wasserbau und Schiffbau, Nr. 13, 1933. See, Rouse's Engineering Hydraulics, 1950, p. 537.
U.S. Waterways Experiment Station, Technical Report; Vibration, Pressure and Air-demand Test in Flood-control Sluice, Pine Flat Dam, Kings River, California. 1954.

2) G. Pajer; Ueber der Strömmungsvorgang an einer unterströmten scharfkantigen Planschütze. ZAMM, 1937 H. 5.
Koch-Carstanjen, Bewegung des Wassers. p. 100.

3) Koch-Carstanjen, 〃 〃

4) S. Uchida; An approximate method for the boundary-value problems by means of the curvilinear coordinates. Report of the Institute of Science and Technology, Univ. of Tokyo, 1. 101, 1947.

5) Goldstein, Modern Developments in Fluid Dynamics. vol. 1, 1938. p. 101

6) See, H. Rouse; Engineering Hydraulics. 1950. p. 539.

(昭. 31. 1. 23)